DOI:10.11835/j.issn.2096-6717.2020.084 开放科学(资源服务)标识码(OSID):

Large deformation finite element analysis of cone penetration tests in calcareous sands

PEI Huimin[1], WANG Dong[1], LIU Qingbing[2]

(1. Shandong Provincial Key Laboratory of Marine Environment and Geological Engineering, Ocean University of China, Qingdao 266100, Shandong, P. R. China; 2. Three Gorges Research Center for Geo-hazard, Ministry of Educations, China University of Geosciences, Wuhan 430074, P. R. China)

Abstract: The cone penetration test (CPT) is widely used to determine the mechanical properties of cohesionless soils. Most of the existing correlations were established in terms of silica sands, while the data for calcareous sands are limited. In comparison to silica sands, calcareous sands have a higher peak internal friction angle and the variation of the friction angle and the dilation angle with strain in calcareous sands is also different from silica sands. In this paper, the Arbitrary Lagrangian Eulerian method and a large deformation finite element approach, was used to study cone penetration in calcareous and silica sands. Frequent mesh generations were conducted to avoid the distortion of soil elements around the cone tip. A modified Mohr-Coulomb constitutive model was introduced to describe the mobilized strength varied with the plastic shear strain in calcareous and silica sands. The elastic and plastic parameters were determined by bender element tests and drained triaxial tests. Numerical results of cone tip resistance agree reasonably well with the existing data from centrifuge tests, showing that the established numerical model has the potential to simulate the cone penetration in calcareous sands.

Keywords: cone penetration tests; calcareous sands; finite element method; large deformation analysis

钙质砂中静力触探试验的大变形有限元模拟

裴会敏[1],王栋[1],刘清秉[2]

(1. 中国海洋大学 山东省海洋环境地质工程重点实验室,山东 青岛 266100;2. 中国地质大学 教育部长江三峡库区地质灾害研究中心,武汉 430074)

摘 要:静力触探试验(CPT)被广泛用于确定无黏性土的力学性质,现有研究集中在普通石英砂,由 CPT 贯入阻力推测钙质砂强度特性的成果很少。钙质砂的峰值内摩擦角一般高于石英砂,内摩擦角和剪胀角随应变的变化也不同于石英砂。采用任意拉格朗日欧拉公式的大变形有限元方法,模拟石英砂和钙质砂中 CPT 的完整贯入过程,有效避免了锥尖周围的网格扭曲。引入修正摩尔-库伦模型描述石英砂和钙质砂强度发挥与塑性剪应变的关系,由弯曲元和三轴排水试验确定本构模型参数。数值模拟得到的锥尖贯入阻力与离心机试验结果吻合,表明建立的数值模型能够模拟钙质砂中的 CPT 试验。

关键词:静力触探试验;钙质砂;有限元;大变形分析

中图分类号:TU433 **文献标志码**:A **文章编号**:2096-6717(2021)01-0048-06

Received:2020-06-04

Foundation items:National Natural Science Foundation of China (No. 41772294, U1806230)

Author brief:PEI Huimin (1996-), main research interest: marine geotechnical engineering, E-mail: peihuimin@stu.ouc.edu.cn. WANG Dong (corresponding author), professor, E-mail: dongwang@ouc.edu.cn.

1 Introduction

The cone penetration test (CPT) is arguably the most important in-situ test in geotechnical investigation. The measured cone resistance can be used to estimate soil properties and pile tip resistance. The analytical approaches used in studying the cone penetration in sands include bearing theories by limit plasticity or slip-line analysis, cavity expansion theories and strain path method[1-3]. Numerically, Mahmoodzadeh et al., Huang et al. and Ahmadi & Dariani reproduced the CPT using different finite element approaches[4-6]. The model tests in the calibration chamber were conducted as well, to validate the above theoretical and numerical results[7].

Most existing studies on the CPT in sands have focused on ordinary silica sands, and studies on the practical applications of CPT in calcareous sands are very limited. Calcareous sands are composed of calcium carbonate particles originating from sedimentation or chemical precipitation, and commonly appear between 30°N latitude and 30°S latitude. Compared with silica sands, features of calcareous sands include an inner pore, more irregular shapes, cementation and particle breakage. Calcareous sands have higher internal friction angles[8], but particle breakage may cause greater strength reduction. It is still not clear if the cone penetration resistance in calcareous sand follows a similar tendency to that of silica sands.

The aim of this paper was to reproduce the CPT in calcareous sands using a large deformation finite element approach. A modified Mohr-Coulomb constitutive model was adopted, considering the strain-softening and elastic stiffness to be varied by stress level. The CPT in silica sands is replicated as well, for comparison.

2 Methodology

2.1 ALE technique

The Arbitrary Lagrangian Eulerian (ALE) function in commercial finite element package Abaqus was used to simulate the cone penetration. The Arbitrary Lagrangian Eulerian technique combines the Lagrangian and Eulerian steps, allowing the mesh to move independently of the material, leaving the remaining mesh topology unchanged. The equilibrium equations, boundary conditions, external loads and contact conditions are satisfied, as in conventional Lagrangian analyses, followed by relocating the nodes and remapping all variables from the old mesh to the new mesh[9]. Therefore, a high-quality mesh is maintained when large deformations occur. Since the far-field soil elements are not seriously distorted during the entire cone penetration, the ALE technique was applied to soil elements around the cone only.

2.2 Soil models

The CPTs in silica or calcareous sands are performed under nearly drained conditions. The total stress analysis is thus sufficient to reproduce the soil response. The soil around the cone undergoes large deformation, and the traditional Mohr-Coulomb model with fixed internal friction angle φ and dilation angle ψ cannot capture the evolution of the mobilized soil strength. Therefore, the Mohr-Coulomb model was modified here to describe the strain-softening response of medium dense or dense sands under drained conditions. The elastic response was captured by Poisson's ratio and elastic shear modulus G as a function of the stress level and void ratio. Poisson's ratio was selected empirically as 0.3 for both silica and calcareous sands.

2.2.1 Shear modulus of sands

The CPT in two sands, KW sand and UWA sand, is studied through ALE analysis incorporating the modified Mohr-Coulomb model. The KW sand is natural calcareous sand from Perth, Australia. Although the calcareous sands spreading in a number of onshore and offshore areas are vulnerable to particle breakage, it was not

found in the centrifuge tests with KW sands[10]. The UWA sand is commercial fine silica sand widely used in the physical model tests at the University of Western Australia. The maximum and minimum void ratios of KW sand are $e_{max}=1.42$ and $e_{min}=0.89$, while $e_{max}=0.78$ and $e_{min}=0.49$ for UWA sand. The particle size distributions of KW sand and UWA sand are given in Fig. 1.

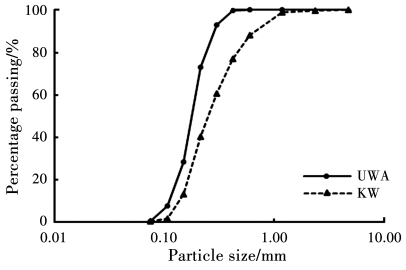

Fig. 1 Particle size distributions of KW sand and UWA sand

The maximum shear modulus G_0 of KW sand and UWA sand are determined through the bender element tests. For KW sand, Fig. 2 shows the variation of the normalized maximum shear modulus with the normalized mean effective pressure, p'/p_a, where p_a is the atmospheric pressure. The maximum shear modulus is usually regarded as a function of the void ratio e and p'[11]. The testing data in Fig. 2 can be fitted as

$$G_0 = 233\frac{(4-e)^2}{1+e}\left(\frac{p'}{p_a}\right)^{0.6}p_a \quad (1)$$

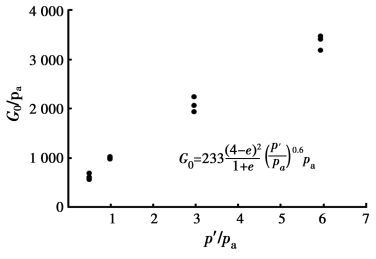

Fig. 2 Small-strain shear modulus of KW sand

Chow et al. reported that the testing results of G_0 of UWA sand can be expressed as[12]

$$G_0 = 1\,000\frac{(1.7-e)^2}{1+e}\left(\frac{p'}{p_a}\right)^{0.5}p_a \quad (2)$$

The maximum shear modulus G_0 refers to strains at $10^{-7}\sim10^{-6}$, while the shear modulus G at relatively large strains is smaller. Papadimitriou et al. and Loukidis & Salgado proposed the degradation of the shear modulus as $G=G_0/T$, where T is the degradation factor[13-14]. Here, the value of T is determined by back-analyzing a centrifuge test in Liu & Lehane[10]: the test for dense sand, KW-1 in Table 1, was simulated using the ALE analysis, and the degradation factor was calibrated as $T=2.5$. Similarly, the degradation factor of the UWA sand was determined as $T=1.54$ through the test of UWA-1 in Table 1.

Table 1 Centrifuge test of CPTs in sands by Liu & Lehane[10]

Test	Sample	Dry density ρ/(kg·m^{-3})	Relative density D_r/%	Cone diameter d/mm	Acceleration level/g
KW-1	KW sand	1 310	70	7	40
KW-2	KW sand	1 310	70	7	80
UWA-1	UWA sand	1 710	78	7	40
UWA-2	UWA sand	1 710	78	7	80

2.2.2 Friction angle and dilation angle

It was assumed that both φ and ψ varied with the equivalent plastic shear strain γ_p, as shown in Fig. 3. φ_i, φ_p and φ_{cv} are the initial, peak and critical internal friction angle, respectively and γ_{p1}, γ_{p2}, γ_{p3}, and γ_{p4} are corresponding threshold equivalent plastic strains. The dilation angle ψ was assumed to be 0.1°, a small value near zero, until the equivalent plastic shear strain reaches γ_{p1}, and then it increased to the peak value ψ_p quickly at γ_{p2}. Similar models[15-17] were used by Potts et al., Hu et al. and Troncone. In this paper, $\gamma_{p1}=0.01$, $\gamma_{p2}=0.012$, $\gamma_{p3}=0.05$ and $\gamma_{p4}=0.15$ were selected for both silica and calcareous sands without considering particle breakage.

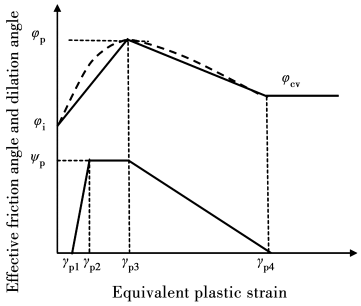

Fig. 3 Schematic diagram of modified Mohr-Coulomb model

Drained triaxial tests are used to determine the friction angle and dilation angle. 1) According to 12

drained triaxial compression tests of KW sand under different relative densities and confining pressures, the critical friction angle $\varphi_{cv} = 36°$ is determined. $\varphi_p = 41°$ and $\psi_p = 6.2°$ for the KW sand with a relative density $D_r = 68\%$ and confining pressure of 100 kPa. Both relative density and stress level are close to the centrifuge test conditions conducted by Liu & Lehane[10]. 2) For UWA sand, Chow et al.[12], conducted drained triaxial tests, with results of $\varphi_{cv} = 31.9°$, $\varphi_p = 42°$ and $\psi_p = 18°$ can be estimated by the stress-dilatancy relationship of UWA sand. The stress-dilatancy relationship can be expressed as Eqs. (3) ~(5).

$$I_R = D_r(6.07 - \ln p'_p) + 1.27 \quad (3)$$

$$\varphi'_p - \varphi'_{cv} = 2.64 I_R \quad (4)$$

$$\varphi'_p - \varphi'_{cv} = 0.55\psi_p \quad (5)$$

where I_R is the relative dilatancy index, and p'_p is the mean effective stress at peak strength, with the units of kPa. The φ'_{cv} value of KW sand was remarkably higher than almost all silica sands, which is consistent with Coop[8].

3 Finite element results and discussion

Four cone penetration tests in centrifuge were performed by Liu & Lehane[10], as listed in Table 1. A 7 mm cone was tested at $40g$ and $80g$, with the corresponding prototype diameter of $d = 0.28$ m and 0.56 m, respectively. The finite element model is shown in Fig. 4. The tip angle was 60°. In the ALE simulations, the soil model was $16d$ wide and $50d$ deep, which was proved to be sufficient to avoid boundary effects. The penetrometer was modelled as a rigid body, as the stiffness of the penetrometer is much greater than that of soil. By following Mahmoodzadeh et al.[4], a smooth rigid tube between the cone and soil was set, which moved together with the cone[5]. The soil elements on the left boundary were to move outwards rather than inwards. The interface between the cone and the sand was simulated with the Coulomb friction law and the interface friction angle was taken as 50% of the critical internal friction angle. The interface between the sleeve and the sand was assumed as smooth, to obtain the cone resistance easily. The lateral earth pressure coefficient $K_0 = 1 - \sin\varphi_{cv}$ and the cone was penetrated with a velocity of 0.016 m/s. The soil was discretized as four-node axisymmetric elements with reduced integration.

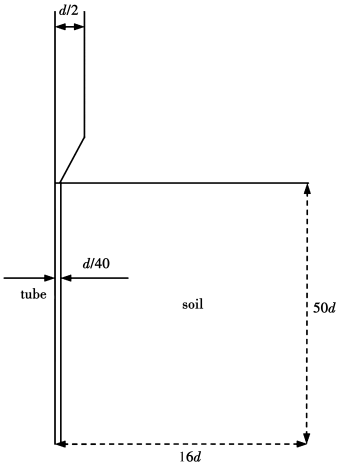

Fig. 4 Sketch of the finite element model

Results of the ALE analyses and centrifuge tests for KW sand and UWA sand are compared in Fig. 5(a) and (b), respectively. q_c is the base resistance and w is the penetration depth in the figure. A good agreement between the numerical and experimental data is achieved, suggesting that the modified Mohr-Coulomb model has the potential to capture the basic behaviors of both the UWA and KW sands. The percentage of particles finer than 1 mm is more than 95% for KW sand (see Fig. 1), so the particle breakage of such fine sand sample was not observed in the centrifuge tests. It is not clear if the modified Mohr-Coulomb can be used for calcareous sands with strong particle breakage.

In Fig. 5, the cone resistance q_c is increased nearly linearly with the penetration depth at the depth larger than $10d$. Compared to UWA sand, the q_c in KW sand is remarkable lower when penetrating at the same depth although the φ_{cv} of KW sand is higher than that of UWA sand. Given

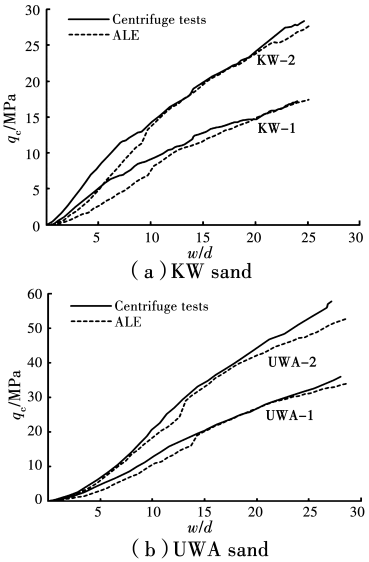

Fig. 5 Comparison between centrifuge tests and ALE results

a similar relative density, the void ratio of UWA sand is smaller than that of KW sand due to the smaller limit void ratio so that the effective density of the UWA sand is larger. Also, the shear modulus of the UWA sand is larger than that of the KW sand. For the KW sand, the degradation factor $T=2.5$ is larger than that of the UWA sand. If $T=1.54$ is employed for the KW sand, the cone resistance would be increased remarkably (see Fig. 6). For both the KW and UWA sands, the mobilized friction angle and the dilation angle around the cone are varied with the plastic strain, gradually approaching the critical values (Fig. 7 and 8). The contour of the equivalent plastic strain in Fig. 7(c) and Fig. 8(c) shows that the plastic zone around the penetrometer is similar to those illustrated in Huang et al. The plastic zone is expanded gradually and moves downwards with the cone[5].

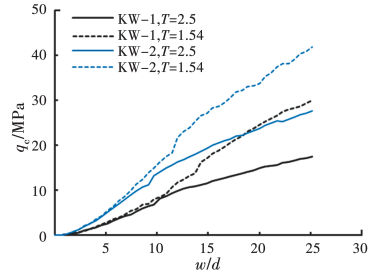

Fig. 6 Influence of stiffness degradation factor on cone resistance for KW sand

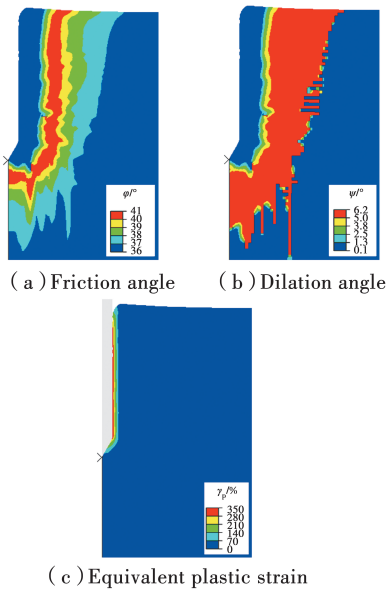

Fig. 7 Simulation results of cone penetration in KW-1 at $z=7d$

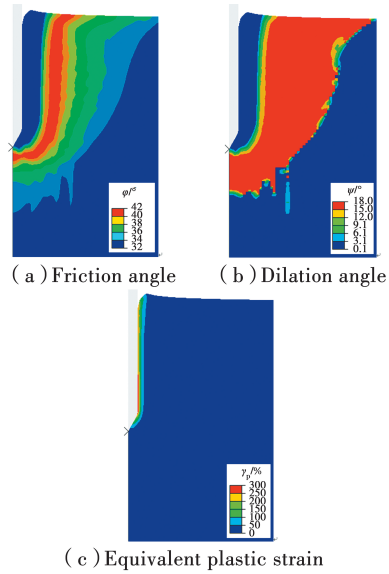

Fig. 8 Simulation results of cone penetration in UWA-1 at $z=7d$

4 Conclusions

The cone penetration in silica and calcareous sands was investigated using the Arbitrary Lagrangian Eulerian method. A modified Mohr-Coulomb model was employed to describe the strength evolutions of silica and calcareous sands, with the soil properties determined through bender element and drained triaxial tests. The variation of the cone resistance with penetration depth was obtained for different stress levels. A relatively good agreement between the numerical and

experimental cone resistance profiles was achieved, suggesting that the modified Mohr-Coulomb model is suitable for calcareous sands without strong particle breakage.

Acknowledgements

The authors would like to acknowledge the financial support from the National Natural Science Foundation of China (Grant No. 41772294, U1806230).

References:

[1] JANBU N, SENNESET K. Effective stress interpretation of in situ static penetration tests [C]// Proceedings of the 1st European Symposium on Penetration Testing. 1974, 2: 181-93.

[2] SALGADO R, MITCHELL J K, JAMIOLKOWSKI M. Cavity expansion and penetration resistance in sand [J]. Journal of Geotechnical and Geoenvironmental Engineering, 1997, 123(4): 344-354.

[3] BALIGH M M. Strain path method [J]. Journal of Geotechnical Engineering, 1985, 111(9): 1108-1136.

[4] MAHMOODZADEH H, RANDOLPH M, WANG D. Numerical simulation of piezocone dissipation test in clays [J]. Geotechnique, 2014, 64(8): 657-666.

[5] HUANG W, SHENG D, SLOAN S W, et al. Finite element analysis of cone penetration in cohesionless soil [J]. Computers and Geotechnics, 2004, 31(7): 517-528.

[6] AHMADI M M, GOLESTANI DARIANI A A. Cone penetration test in sand: A numerical-analytical approach [J]. Computers and Geotechnics, 2017, 90: 176-189.

[7] HOULSBY G T, HITCHMAN R. Calibration chamber tests of a cone penetrometer in sand [J]. Geotechnique, 1988, 38(1): 39-44.

[8] COOP M R. The mechanics of uncemented carbonate sands [J]. Geotechnique, 1990, 40(4): 607-626.

[9] WANG D, BIENEN B, NAZEM M, et al. Large deformation finite element analyses in geotechnical engineering [J]. Computers and Geotechnics, 2015, 65: 104-114.

[10] LIU Q B, LEHANE B M. A centrifuge investigation of the relationship between the vertical response of footings on sand and CPT end resistance [J/OL]. Géotechnique, 2020: 1-11. http://doi.org/10.1680/jgeot.19.P.253.

[11] HARDIN B O, BLACK W L. Sand stiffness under various triaxial stresses [J]. Journal of the Soil Mechanics and Foundations Division, 1966, 92(2): 27-42.

[12] CHOW S H, ROY A, HERDUIN M, et al. Characterisation of UWA superfine silica sand [R]. 2019.

[13] PAPADIMITRIOU A G, BOUCKOVALAS G D, DAFALIAS Y F. Plasticity model for sand under small and large cyclic strains [J]. Journal of Geotechnical and Geoenvironmental Engineering, 2001, 127(11): 973-983.

[14] LOUKIDIS D, SALGADO R. Modeling sand response using two-surface plasticity [J]. Computers and Geotechnics, 2009, 36(1/2): 166-186.

[15] POTTS D M, KOVACEVIC N, VAUGHAN P R. Delayed collapse of cut slopes in stiff clay [J]. Geotechnique, 1997, 47(5): 953-982.

[16] HU P, WANG D, STANIER S, et al. Assessing the punch-through hazard of aspudcan on sand overlying clay [J]. Geotechnique, 2015, 65(11): 883-896.

[17] TRONCONE A. Numerical analysis of a landslide in soils with strain-softening behaviour [J]. Geotechnique, 2005, 55(8): 585-596.

(编辑 章润红)